J Neurophysiol 96: 2995–3005, 2006.
First published August 30, 2006; doi:10.1152/jn.00061.2006.

Intraspinal Microstimulation Excites Multisegmental Sensory Afferents at Lower Stimulus Levels Than Local α-Motoneuron Responses

R. A. Gaunt,[1] A. Prochazka,[1] V. K. Mushahwar,[1] L. Guevremont,[1] and P. H. Ellaway[2]
[1]*Department of Biomedical Engineering and Center for Neuroscience, University of Alberta, Edmonton, Alberta, Canada; and* [2] *Division of Neuroscience and Mental Health, Imperial College London, London, United Kingdom*

Submitted 19 January 2006; accepted in final form 26 August 2006

Gaunt, R. A., A. Prochazka, V. K. Mushahwar, L. Guevremont, and P. H. Ellaway. Intraspinal microstimulation excites multisegmental sensory afferents at lower stimulus levels than local α-motoneuron responses. *J Neurophysiol* 96: 2995–3005, 2006. First published August 30, 2006; doi:10.1152/jn.00061.2006. Microstimulation within the motor regions of the spinal cord is often assumed to activate motoneurons and propriospinal neurons close to the electrode tip. However, previous work has shown that intraspinal microstimulation (ISMS) in the gray matter activates sensory afferent axons as well as α-motoneurons (MNs). Here we report on the recruitment of sensory afferent axons and MNs as ISMS amplitudes increased. Intraspinal microstimulation was applied through microwires implanted in the dorsal horn, intermediate region and ventral horn of the L_5–L_7 segments of the spinal cord in four acutely decerebrated cats, two of which had been chronically spinalized. Activation of sensory axons was detected with electroneurographic recordings from dorsal roots. Activation of MNs was detected with electromyographic (EMG) recordings from hindlimb muscles. Sensory axons were nearly always activated at lower stimulus levels than MNs irrespective of the stimulating electrode location. EMG response latencies decreased as ISMS stimulus intensities increased, suggesting that MNs were first activated transsynaptically and then directly as intensity increased. ISMS elicited antidromic activity in dorsal root filaments with entry zones up to 17 mm rostral and caudal to the stimulation sites. We posit that action potentials elicited in localized terminal branches of afferents spread antidromically to all terminal branches of the afferents and transsynaptically excite MNs and interneurons far removed from the stimulation site. This may help explain how focal ISMS can activate many MNs of a muscle even though they are distributed in long thin columns.

INTRODUCTION

For the past 10 years, intraspinal microstimulation (ISMS) has been explored as a means of restoring limb movement and bladder control after spinal cord injury (Barbeau et al. 1999; Carter et al. 1995; McCreery et al. 2004; Mushahwar and Horch 1997, 1998). However, ISMS is in its infancy as a rehabilitation technique and many details surrounding the mechanisms by which ISMS affects activity in the spinal cord and recruits neurons have not been systematically studied.

In understanding the mechanism of action of ISMS, it is important to know the extent to which ISMS recruits different populations of axons as well as neuronal cell bodies. If large numbers of sensory axons were recruited at lower stimulus intensities than motoneuronal cell bodies or axons, their synaptic action on interneurons as well as motoneurons could greatly affect the motor outcome. As Nowak and Bullier (1998) pointed out "The question that arises is: When a postsynaptic response is obtained after the stimulation of the gray matter, what are the presynaptic neuronal elements activated? The answer to that question is essential, because it will determine the interpretation of the results obtained."

ISMS was first used as an experimental tool to measure α-motoneuron (MN) synaptic delay to test whether the reflexive activation of MNs by dorsal root stimulation was monosynaptic (Renshaw 1940). Renshaw showed that at low stimulus strengths, MNs were activated transsynaptically, and at higher strengths, they were activated directly. Along similar lines, Jankowska et al. (1975) found that of all the pyramidal tract cells activated with weak microstimulation of the motor cortex in cats and monkeys, only about one-third were activated directly. Gustafsson and Jankowska (1976) did a more detailed study of ISMS in cats in which they concluded that MNs were activated directly when the microelectrode tips were adjacent to the initial segment of the MN axon or adjacent to the soma. However, when the tips were among MN dendrites and at more distant locations from the soma, MNs were activated transsynaptically. Additional work from the same group has also demonstrated the very low activation thresholds of axons in the CNS (Jankowska and Roberts 1972; Roberts and Smith 1973).

ISMS has been used by Bizzi and colleagues to study the organization of spinal neural circuitry controlling limb movement (Bizzi et al. 1991). ISMS in the gray matter of the lumbosacral spinal cord of decerebrate frogs elicited isometric forces in the hindlimb that converged to discrete points. This led to the hypothesis of "movement primitives" in which the spinal cord was suggested to contain four or five basic neural modules producing elemental synergies that could be combined to produce a wide range of movements (Bizzi et al. 1991, 2002; Giszter et al. 1993). In his critique of the concept of movement primitives, Loeb (1992) suggested that the only known topographic structures in the spinal cord are elongated, columnar entities that could not be selectively activated by single microelectrodes. However, Bizzi et al. always assumed that focal ISMS activated sets of interneurons that projected to and activated MN pools in an organized way. From the work of Renshaw and Jankowska and colleagues, one would have expected that sensory afferents would be activated by ISMS, adding synaptic input to MNs. Yet in two sets of experiments, ISMS-evoked movement primitives were reported to be similar

Address for reprint requests and other correspondence: R. A. Gaunt, Dept. of Biomedical Engineering and Center for Neuroscience, University of Alberta, 507 HMRC, University of Alberta, Edmonton AB, T6G 2S2, Canada (E-mail: rgaunt@ualberta.ca).

The costs of publication of this article were defrayed in part by the payment of page charges. The article must therefore be hereby marked "*advertisement*" in accordance with 18 U.S.C. Section 1734 solely to indicate this fact.

before and after chronic deafferentation (Giszter et al. 1993; Tresch and Bizzi 1999). As well, microiontophoretically applied *N*-methyl-D-aspartate (NMDA), which activates cell bodies directly, often produced synergies similar to those produced by ISMS in the same locations (Saltiel et al. 2001). It was argued from these experiments that convergent force fields elicited by ISMS were the result of activating local neurons directly rather than indirectly through incoming axons (Bizzi et al. 1995). Other studies have suggested a modular organization within the dorsal horn of the spinal cord specifically to process cutaneous afferent nociceptive stimuli to coordinate the classical withdrawal reflex (Levinsson et al. 1999; Schouenborg 2003; Schouenborg and Kalliomaki 1990; Schouenborg et al. 1992).

Our study was designed to examine the order of recruitment of sensory afferents and MNs (axons or cell bodies), to reveal the rostrocaudal extent of the antidromically activated sensory responses, and to characterize and compare the resultant synaptic and direct activation of limb muscles. We found that ISMS at a single point in the spinal cord gray matter activated afferent terminals along the entire length of the lumbosacral enlargement. This casts a new light not only on the mechanism of action of ISMS as a clinical tool, but also on the interpretation of ISMS studies of the organization of the motor elements of the spinal cord. Preliminary results of the present study have been reported in abstract form (Mushahwar et al. 2003).

METHODS

This report is based on four acute experiments performed to test two hypotheses. *1*) As the amplitude of ISMS pulses is increased, afferent axons are activated at lower amplitudes than MNs. *2*) Antidromic potentials in sensory afferents have multisegmental reflex effects. Two spinally intact cats (*R3* and *R4*) and two chronically spinalized cats (*R1* and *R2*) were used. Chronic spinalizations were performed to minimize the effects of acute decerebration on the state of the spinal cord and to study ISMS after spinal cord injury, a condition for which ISMS has been proposed as a rehabilitative strategy. The experiments were done with the approval of the University of Alberta Animal Research Ethics Committee.

Surgical procedure

SPINALIZATION. The cats were anesthetized with ketamine (25 mg/kg im) and intubated using an infant tracheal tube. Preoperative medication was administered: acepromazine (0.25 mg/kg im), glycopyrrolate (0.01 mg/kg im), and buprenorphine (0.01 mg/kg sc). In addition, the antibiotic cefazolin was administered (10 mg/kg iv). The animal's back was shaved, washed with warm soap and water, and scrubbed with iodine solution (betadine). Anesthesia was maintained with isoflurane (2–3% in carbogen, flow rate: 1,500 ml/min). A slow intravenous drip of sterile Ringer solution was administered to maintain fluid balance.

The skin was incised over the T_{10}–L_1 spinous processes, and a laminectomy was performed at the T_{10}/T_{11} vertebral junction. The dorsal aspect of the dura mater was incised transversely, and a solution of 2% lidocaine (0.2 ml) was dripped on the surface of the cord. Two minutes later, lidocaine was injected into the spinal cord at progressively more ventral levels. Fine scissors were used to transect the cord. The transection was carefully verified visually with a surgical microscope, and a hemostatic mesh, Surgicel (Ethicon, Somerville, NJ), was placed in the gap created by the sectioned spinal cord. The dura mater was sutured shut and the incision was closed in layers. At extubation, the cat was given ketoprofen (2.0 mg/kg sc). Analgesia was maintained as necessary with ketoprofen (2.0 mg/kg sc) or buprenorphine (0.01 mg/kg sc). Cefazolin was administered for 4 days after surgery, followed by amoxicillin (50 mg tablets, 2/day) for 6 additional days. During postoperative recovery, the cats were kept warm in heated cages provided with blankets. The animals were allowed to recover for 6–8 wk before the terminal experiment.

TERMINAL EXPERIMENT. In each experiment, the cat was initially anesthetized with the gaseous anesthetic isoflurane (2–3% in carbogen, flow rate 2 l/min). A tracheotomy was performed, and a tracheal tube was inserted to allow control of ventilation with a closed-loop anesthetic machine. The carotid artery was ligated on one side and catheterized on the other to allow monitoring of blood pressure. The jugular vein was catheterized to allow drug administration.

A laminectomy was performed to expose the L_5–S_1 region of the spinal cord and associated dorsal roots after which the cat was fixed in a stereotaxic frame. An array of four to six microwires was inserted through the dura mater into the L_5–L_7 spinal cord (*R1*: 4 electrodes in L_6–L_7; *R2*: 6 electrodes in L_6; *R3*: 6 electrodes in L_5; *R4*: 6 electrodes in L_6). The microwires were made from 25- or 30-μm-diam stainless steel insulated with polyimide with 60–100 μm of wire bared at the tip and cut with a sharp scalpel blade to have an acutely angled bevel. Once the wires were inserted into the spinal cord, the array was fixed to the dura mater and the L_3 spinous process with droplets of Loctite 420 cyanoacrylate glue. The depths of insertion of the microwires from the cord dorsum ranged from 1.75 to 3.5 mm, targeting the dorsal horn (lamina IV, V, VI), intermediate gray matter (lamina VII), and the ventral horn (lamina IX). The locations of the electrode tips established in postmortem dissections of the spinal cord are shown in Fig. 1. Electrode positions were identified by serial sectioning of the formalin-fixed spinal cord. Once an electrode was visualized, the size and shape of the white and gray matter were recorded as well as the position of the electrode tip within the gray matter. In *cat R4,* the ISMS electrodes were dislodged from the spinal cord at the termination of the experiment. However, based on this and previous work, we are confident that these electrodes were within the gray matter and evenly distributed from the dorsal to ventral horn.

Bipolar EMG electrodes (Cooner AS631) were implanted in five to eight of the following hindlimb muscles ipsilateral to the ISMS electrodes: lateral gastrocnemius (LG), medial gastrocnemius (MG), tibialis anterior (TA), biceps femoris posterior (BFp), biceps femoris anterior (BFa), vastus lateralis (VL), sartorius anterior (Sart), and semimembranosus anterior (SMa). The inter-electrode spacing was ~2 cm. The hip, knee, and ankle joints of the leg ipsilateral to the ISMS electrodes were fixed by clamps to the base of the stereotaxic frame to minimize movement during ISMS trials. A heating blanket under the abdomen was used to maintain body temperature. The skin at the laminectomy site was attached to the frame with elastic bands to form a pool that was filled with clear paraffin oil to cover the exposed spinal cord. A heating lamp was used to maintain the temperature of the paraffin oil close to body temperature.

A mid-collicular decerebration was performed and isoflurane anesthesia was discontinued. Decerebration abolishes consciousness but spares basic motor functions mediated by the brain stem and spinal cord. A period of 1–2 h was allowed for the effects of the anesthetic on the spinal cord to wear off. After hindlimb tone and reflexes had re-appeared, ISMS pulses were applied through each of the implanted microwires. Antidromic responses were recorded in cut dorsal root filaments with bipolar platinum hook electrodes. Filaments were selected according to the distance of their cord entry points rostral and caudal to the stimulation sites. MN activation was recorded indirectly in the form of EMG responses in the hindlimb muscles implanted with EMG electrodes. Figure 2 provides a schematic of the experimental setup. Stimulus-response properties of the dorsal root and EMG responses were characterized for a range of ISMS intensities. In one

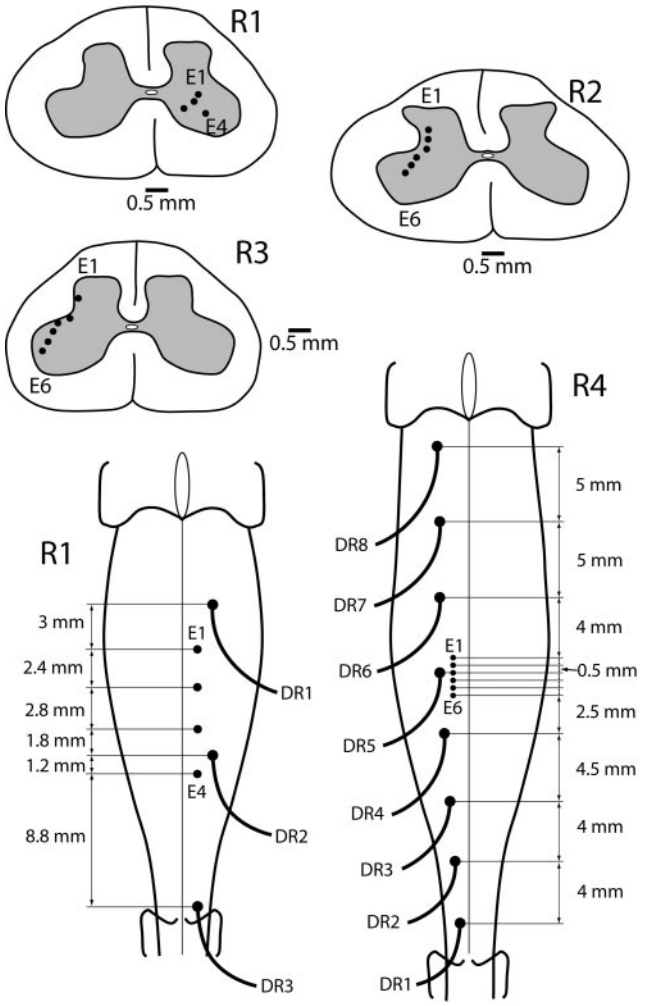

FIG. 1. Electrode locations in 3 of the 4 cats. In addition to the dorsoventral spread shown in the *top half* of the figure, electrodes were distributed rostrocaudally with the most rostral electrode also being the most dorsal and the most caudal electrode also being the most ventral. The rostrocaudal interelectrode spacing was 0.5 mm in *cats R3* and *R4,* 1 mm in *cat R2,* and varied in *cat R1* (see diagram). In *cat R4,* the intraspinal microstimulation (ISMS) electrodes were dislodged from the spinal cord at the conclusion of the experiment and therefore their exact locations could not be verified. The rostrocaudal location of the electrodes in relation to the recorded dorsal rootlets is shown for *cats R1* and *R4* in the *lower half* of the figure. Similar diagrams for *cats R2* and *R3* are shown in Figs. 5 and 6, respectively.

cat, data were obtained under isoflurane anesthesia before decerebration as well as after decerebration in the absence of anesthesia.

Data recording and analysis

RECORDING, SAMPLING, AND STIMULATION. Electroneurograms (ENGs) from the cut dorsal root filaments were amplified with an Iso-DAM8A differential instrumentation amplifier (World Precision Instruments, Sarasota, FL) at a gain of 10,000 and band-pass filtered from 300–3,000 Hz with a 20 db/decade roll-off. Hindlimb EMGs were amplified with Neurolog NL824 preamplifiers and NL820A isolator units (Digitimer, Welwyn Garden City, UK) at a gain of 1,000 and band-pass filtered from 100 to 2,000 Hz with a 20 db/decade roll-off using custom-built filters. All signals were displayed on Tektronix analog oscilloscopes, digitally sampled at 20,000 samples per second and stored with the use of a CED 1401plus Laboratory Interface (Cambridge Electronic Design, Cambridge, UK). Sampling was peri-triggered with 5–20 ms of prestimulus data and 10–20 ms of poststimulus data. Neurolog modules NL304 (period generator), NL403 (delay-width), NL510 (pulse buffer), and NL800 (stimulus isolator) were used to deliver 200-μs-long, constant current monophasic pulses through the ISMS electrodes at 1 pulse/s. Each trial consisted of 50–250 individual records, and this was repeated for each stimulation amplitude. Stimulation amplitudes ranged from 20 to 300 μA depending on the animal and location of the microwire within the spinal cord. The stimulus amplitude was slowly increased from zero until any response was observed visually on oscilloscopes displaying dorsal root ENG and hindlimb muscle EMG waveforms. Sampling was commenced at this amplitude and proceeded at increasing values until both the pattern of ENG and EMG activity did not change appreciably with increased stimulation amplitude or when the stimulation current reached 300 μA.

AUTOMATIC THRESHOLD DETECTION. The primary aim of this study was to compare the stimulus amplitudes first eliciting ENGs and EMGs. The progression of EMG onset response latencies was also of interest. To eliminate qualitative judgment of EMG onset, the presence of activity and its corresponding onset latency was automated using custom software in Matlab v6.5 (The Mathworks, Natick, MA). The data were preprocessed, and any DC offset present in the prestimulus data was removed from each record individually. Each record was then rectified and analysis was resumed.

The two-sample *t*-test was used to detect the onset latencies of ENG and EMG signals. The null hypothesis was that the distribution of data from all records of a given signal at a given poststimulus latency was equal to the distribution of data from all prestimulus times (significance at $P < 0.001$). Each poststimulus latency was tested in this way. Consider a data set in which 80 records of responses to the same stimuli were obtained with 20 ms of prestimulus data and 20 ms poststimulus, sampled at 20,000/s. For each latency, the two distributions for *t*-test analysis would comprise 32,000 prestimulus points and 80 poststimulus points. The first 0.5 ms of poststimulus ENG signal containing the stimulus artifact was neglected as was the first 2 ms of EMG signal (the minimal possible response latency). Finally, the criterion for detecting a response onset was that consecutive data points spanning $\geq$0.5 ms of the ENG signal and $\geq$1 ms of the EMG signal reached significance. The difference in window length for ENG and EMG signals was selected to minimize false positive detections. Because the longer window for EMG activity might bias detection

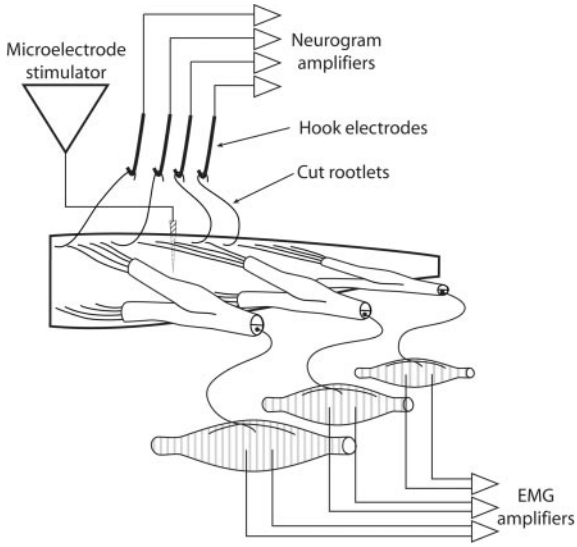

FIG. 2. Schematic of the experimental setup. The locations of ISMS electrodes, dorsal roots, dorsal root recording hook electrodes, and implanted electromyographic (EMG) electrodes are shown. For clarity, only one of the ISMS electrodes is shown.

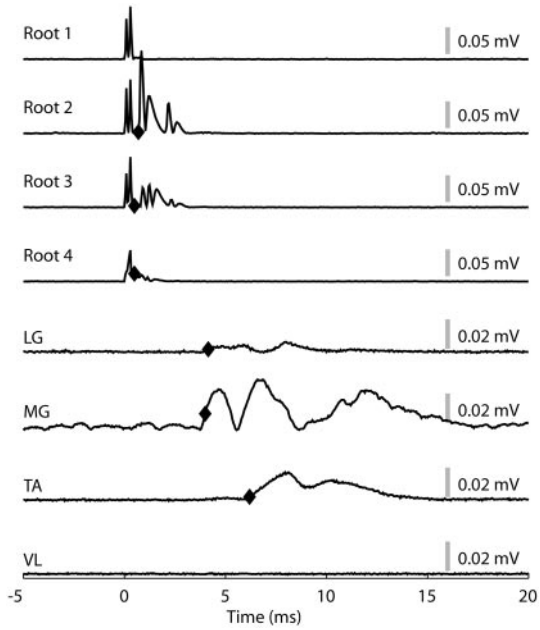

FIG. 3. Averaged dorsal root ENGs (*top 4 traces*) and hindlimb EMGs (*bottom 4 traces*) in response to an ISMS pulse suprathreshold for both sensory and motor responses. The stimulation pulse was delivered at time $t = 0$ s. The ♦ mark the location of automatically detected activity onsets. The large spikes at the beginning of the electroneurographic (ENG) signals are stimulus artifacts. No activity was detected in dorsal root 1 or VL in this case. Note the difference in onset latency between EMG and ENG signals.

toward higher stimulation amplitudes, all collected data were also analyzed with an EMG detection window of 0.5 ms. In this scenario, EMG signals were occasionally detected at lower thresholds; however visual inspection of these data often did not positively identify activity. Additionally, in no case did this change reduce any EMG thresholds to be equal to or less than the ENG thresholds. Because of this, the EMG detection window was left at 1.0 ms.

Figure 3 shows an example of the processing and automatic detection of ENG and EMG signals in one data set. The stimulus artifacts in the ENG signals can be clearly seen and in this example an ENG signal was detected in dorsal roots 2–4. Four of the eight recorded EMG channels are also shown. An EMG signal was detected in LG, MG, and TA but not in VL.

RESULTS

ISMS activates afferent fibers at lower amplitudes than local MN cell bodies or axons

Figure 4 shows an example of a sequence of trials in *cat R3* in which ISMS intensity was increased in steps from 35 to 150 μA. Each trace is an average of responses to ~110–220 stimuli. Six ISMS stimulus intensities are represented. At the lowest intensity, ENG responses are evident in two of the three dorsal root filaments, whereas no EMG responses are seen. As ISMS amplitude was increased, the amplitudes of dorsal root responses increased and EMG responses appeared and grew in amplitude. The data in Fig. 4 were typical of nearly all trials in that dorsal root responses occurred at lower stimulation intensities than EMG responses.

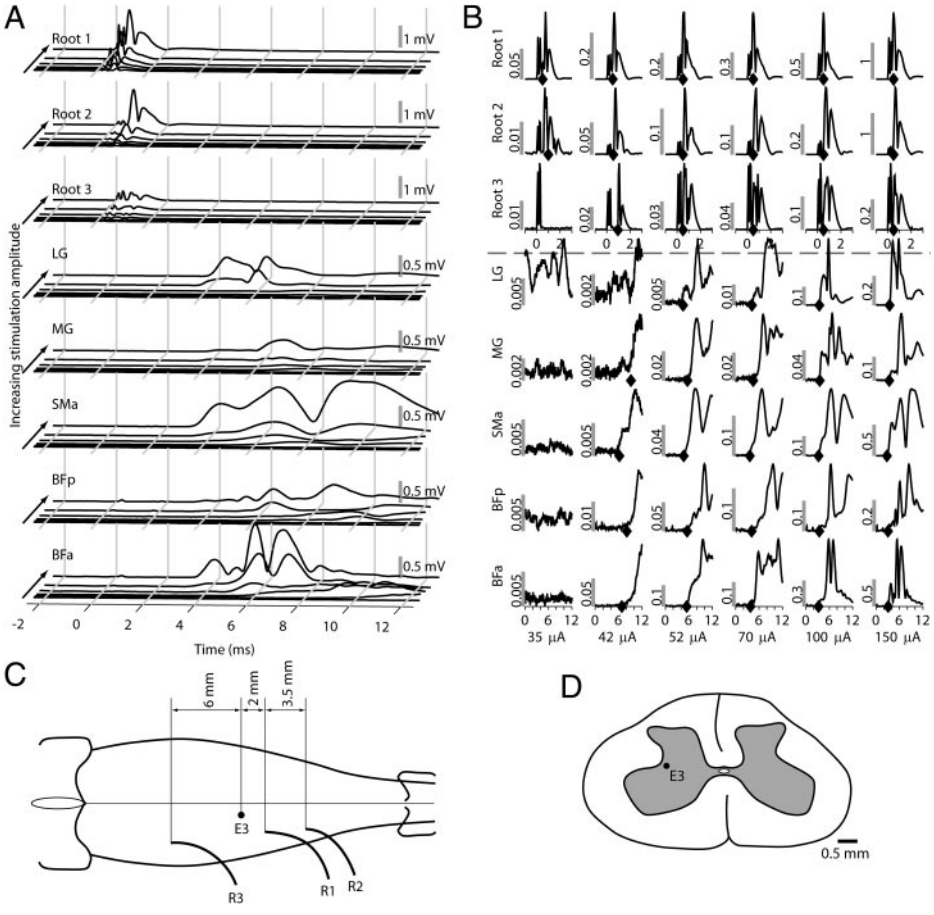

FIG. 4. A sequence of dorsal root ENG and hindlimb EMG responses to increasing stimulation amplitudes through an ISMS electrode in the intermediate region of chronically spinalized *animal R2.* The stimulation amplitude was increased from 35 to 150 μA during the trial. In each case, the plotted trace is the average of ~110–220 stimuli. Each row is labeled with the dorsal root or muscle that the signal was recorded from. This progression of responses was typical among all cats and experimental parameters. *A*: progression of responses plotted on the same vertical scale for the duration of the trial. Stimulation amplitude increases in the direction noted to the left of each panel. The increase in the magnitude of the responses in both the dorsal roots and muscles can be clearly seen. In the muscles, the progression from long-latency responses at low stimulation amplitudes to short-latency responses at higher stimulation amplitudes can also be seen. *B*: data from *A* plotted on varying scales so that the details of the responses can be visualized. Each row is labeled with the dorsal root or muscle the data were recorded from and correspond to the rows of *A*. Each column presents data from different stimulation amplitudes. The amplitude scale is plotted in each panel in millivolts. Note that the time scales for the dorsal root signals and EMG signals are different but are both in milliseconds. ♦, onset of activity in each case where activity was determined to have occurred. At the lowest intensity, responses are evident in 2 of the 3 dorsal root filaments in the absence of detectable EMG responses. As ISMS intensity was gradually increased, the amplitudes of dorsal root responses increased and EMG responses appeared and grew in amplitude. *C*: schematic showing the location of the ISMS electrode (E3) and recorded dorsal rootlets. *D*: cross-section of the spinal cord showing the location of the ISMS electrode tip (E3).

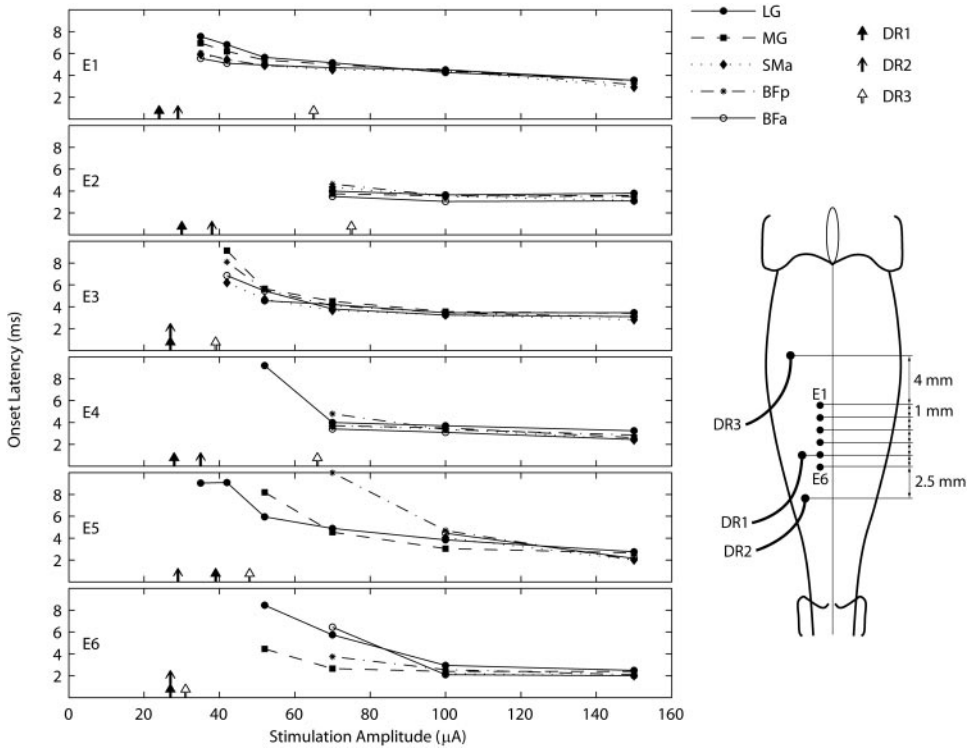

FIG. 5. Stimulation thresholds of the dorsal root ENGs and hindlimb EMGs as well as the latencies of EMG responses for each ISMS electrode in chronically spinalized *cat R2.* Each panel presents the data for 1 of the 6 ISMS electrodes (E1–E6). E1 was the most rostral and dorsal electrode, whereas E6 was the most caudal and ventral electrode. Arrows, indicate the stimulation amplitude at which each of the dorsal roots first exhibited detectable ENGs. Stacked arrows indicate multiple dorsal roots with the same stimulation threshold. The roots are identified by distinctive arrow styles. The onset latencies for each muscle are also displayed as a function of stimulation amplitude. For example, in E5, lateral gastrocnemius (LG) first exhibited detectable activity at a stimulation amplitude of 35 μA and at a latency of 9 ms, whereas medial gastrocnemius (MG) first exhibited detectable activity at a stimulation amplitude of 52 μA and at a latency of 8 ms. The relative location of the stimulation electrodes and the dorsal rootlets recorded from are also shown. Note that in all cases, activity was detected in some dorsal root ENGs at lower stimulation amplitudes than hindlimb EMGs.

Figure 5 presents the complete data set for chronically spinalized *cat R2.* The six panels show response thresholds for dorsal root ENGs and hindlimb muscle EMGs for each of the six microwires through which ISMS was delivered. Electrode E1 was the most dorsal electrode and E6 was the most ventral electrode. The onset latencies for EMG data are also shown. The response thresholds for the three dorsal roots sampled in this cat are indicated by arrows along the *x* axis. EMG responses from each muscle are plotted as response latency versus stimulation amplitude. In this cat, ENG responses were always detected in some dorsal roots before any EMG activity even for the deepest stimulating electrode. The first dorsal root ENG response was detected at a mean stimulus amplitude of 28 ± 2 (SD) μA. One might presume that deeper stimulating electrodes would be closer to MN cell bodies and their axons and thus activate MNs (somatically or axonally) at lower stimulation intensities. However, there was no evidence for this in *cat R2,* even though this progression of responses was observed in other animals (see following text). In fact, even with the deepest electrode, the EMG onset latencies suggest that MNs were first activated indirectly by transsynaptic pathways.

As the stimulation amplitude was increased, it was also generally observed that the EMG response latency decreased in most muscles. Across all animals and all conditions, linear regression of the pooled data indicated that EMG latency did in fact decrease with increasing stimulation amplitude (ANOVA $P < 0.001$). However, $<10\%$ of the variance of pooled data were accounted for by the regression ($r^2 = 0.075$). At the highest ISMS amplitudes, the measured EMG latencies were 3–4 ms when ISMS was delivered through the more dorsal electrodes and gradually decreased to 2 ms for the most ventral electrode. Even though 4 ms is not an unreasonable time for detection of EMG with direct MN stimulation assuming a conduction velocity of 60 mm/ms, 200 mm of axon, and a delay of 0.5 ms at the neuromuscular junction, the decrease in onset latency from dorsal to ventral suggests transsynaptic activation of MNs with the dorsal electrodes. This seems reasonable because no MNs are present in the dorsal horn and estimations of current spread in spinal gray matter from a microelectrode are around 0.5–1 mm at 150 μA (Gustafsson and Jankowska 1976; Ranck 1975; Snow et al. 2006). With this amount of current spread, it is unlikely that MNs could be activated directly. More interestingly, at lower ISMS amplitudes, EMG onset latencies were much higher (4–10 ms), indicating that MNs were almost certainly activated transsynaptically. These responses are likely mediated by at least some of the sensory afferents the antidromic responses of which were recorded in the dorsal roots.

Figure 6 presents the complete data set for *cat R3,* one of the two spinally intact cats, in the same format as Fig. 5. In this cat, the differences between the thresholds of dorsal root ENGs and hindlimb EMGs ranged more widely than those in *R2.* For example, electrode E1 elicited the first dorsal root response at 39 μA, but the first EMG response did not appear until 90 μA. The deeper electrode, E5, elicited the first dorsal root response at 31 μA and the first EMG response at 33 μA. This decrease in EMG threshold as the electrode tips neared MNs is what would be expected from Gustafsson and Jankowska (1976), unlike the findings in *animal R2.* When stimulating through electrode E6, the deepest of the ISMS electrodes, the threshold for TA EMG was 31 μA, whereas the minimum dorsal root ENG threshold was 36 μA. In this instance, hindlimb EMG activity was detected at a lower stimulus intensity than dorsal root ENG activity.

Figure 7 shows a summary of the results obtained from each cat. Afferents were activated at lower thresholds than MNs, the only exceptions being the deepest electrodes in *cats R3* and *R4.*

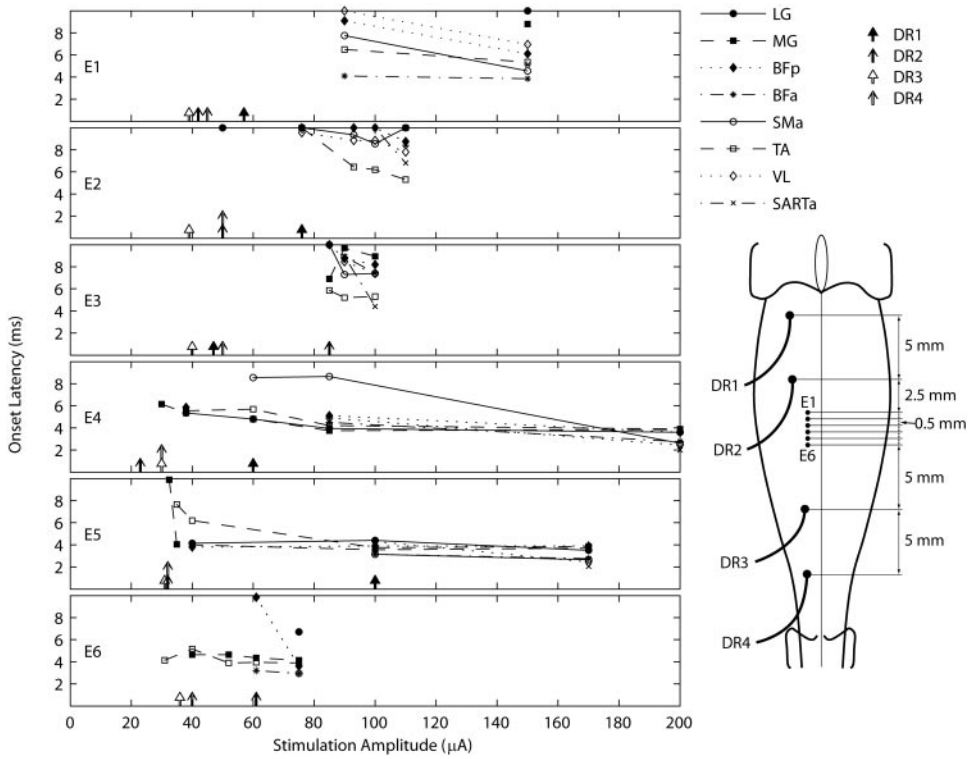

FIG. 6. Stimulation thresholds of the dorsal root ENGs and hindlimb EMGs as well as the latencies of EMG responses for each ISMS electrode in spinally intact *cat R3*. Each panel presents the data for 1 of the 6 ISMS electrodes (E1–E6). E1 was the most rostral and dorsal electrode, whereas E6 was the most caudal and ventral electrode. Arrows indicate the stimulation amplitude at which each of the dorsal roots first exhibited detectable ENGs. Stacked arrows indicate multiple dorsal roots with the same stimulation threshold. The roots are identified by distinctive arrow styles. The onset latencies for each muscle are also displayed as a function of stimulation amplitude. For example, in panel E4, MG first exhibited detectable activity at a stimulation amplitude of 30 μA and at a latency of 6 ms, whereas SMa first exhibited detectable activity at a stimulation amplitude of 60 μA and at a latency of 8.5 ms. The relative location of the stimulation electrodes and the dorsal rootlets recorded from are also shown. Note that in electrodes E1–E5, activity was detected in dorsal root ENGs at lower stimulation amplitudes than hindlimb EMGs.

Even in these cases, the difference in thresholds between the first EMG and first ENG was only 3–5 μA. This implies that in general, ISMS did not activate MNs without also antidromically activating local afferents, whose arborizations extended rostrally and caudally in the spinal cord.

In addition to activating afferent fibers at lower amplitudes than MN cell bodies or axons, ISMS in the spinal gray matter may activate both ascending and descending propriospinal pathways as well as local interneurons. The possible effect of ISMS-activated descending pathways on dorsal rootlet thresholds as well as EMG thresholds and latency at threshold was measured using a Mann-Whitney Rank Sum test to compare the spinally intact group to the chronically spinalized group in which descending contributions are absent. Statistically significant differences were found between the spinal and nonspinal cats in the dorsal rootlet ENG thresholds (intact: 63.6 $\pm$ 40.2 μA; spinalized: 51.4 $\pm$ 20.8 μA, $P = 0.046$) and hindlimb muscle EMG thresholds (intact: 125.2 $\pm$ 71.0 μA; spinalized; 109.9 $\pm$ 70.8 μA, $P = 0.037$) but not in the EMG latency at threshold (intact: 5.8 $\pm$ 3.4 ms; spinalized: 5.3 $\pm$ 2.3 ms, $P = 0.86$). A number of nonneurophysiological explanations may account for these differences. In the spinally intact cats, the rostrocaudal extent of dorsal rootlets recorded from was greater and these distant rootlets generally had higher thresholds. Also, the locations of ISMS electrodes were not consistent between experiments, potentially leading to differences in EMG thresholds not related to the spinal state of the animal.

Spread of focal stimulation in the spinal cord

The rostrocaudal extent to which compound dorsal root action potentials could be recorded was larger than the length of the lumbosacral enlargement. Figure 8 shows the response thresholds of dorsal rootlet ENGs as a function of the rostrocaudal distance between the rootlet entry zone into the spinal cord and the ISMS electrode. The data from all four cats are combined in Fig. 8*A*. The most striking feature of this plot is the $\pm$17 mm extent of dorsal root responses to focal ISMS (farther distances were not explored).

Figure 8 shows that as the distance from the stimulation location (shown as 0) increased, the average stimulation amplitude required to elicit a response in the dorsal roots increased. Dorsal rootlets entering the spinal cord at the position of the ISMS electrode and $\leq$5 mm caudally all exhibited detectable ENGs between 24 and 43 μA. Caudally, the stimulation threshold to elicit ENGs increased to 62–214 μA for dorsal roots 15–17 mm from the stimulating electrode site. Rostrally, the stimulation threshold to elicit ENGs was 30–110 μA for dorsal roots 15–17 mm from the stimulating electrode with the exception of a single outlying point. For typical ISMS amplitudes (50–250 μA) used to generate functional movement with microwires of the type we used (Mushahwar et al. 2000), afferent backfiring would cause the focally applied stimulation to excite regions of the spinal cord up to at least $\pm$17 mm away from the stimulation site. Note that $\pm$17 mm refers to the most rostral and caudal dorsal root entry points. Figure 8*B* presents the same data as Fig. 8*A*, but the spread elicited by each electrode for each cat can be individually seen. To examine potential differences between the anesthetized and decerebrate case in *animal R4,* both linear and quadratic regression lines were fitted to each of these data sets. The regression lines were compared using an *F* test and in neither case ($P = 0.88$ linear, $P = 0.89$ quadratic) was there a significant difference between the anesthetized and decerebrate state. Additionally, no obvious relationship between the stimulating electrode depth and the dorsal rootlet ENG threshold at different rostrocaudal locations was found. The fourth panel of Fig. 8*B* (*R4*-IA) shows that the dorsal rootlet 15–17 mm caudal

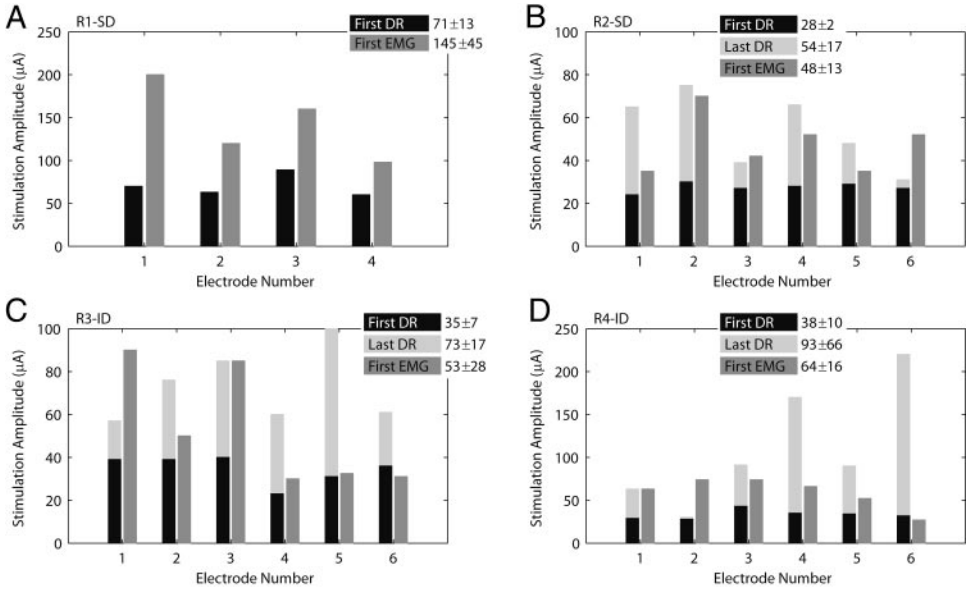

FIG. 7. Differences between stimulation amplitude required to elicit dorsal root ENGs and hindlimb EMGs depending on the stimulating electrode. The first DR" response was the minimum stimulation amplitude at which compound action potentials were recorded from any of the dorsal roots. The "Last DR" response was the minimum stimulation amplitude at which action potentials were recorded on all dorsal roots. The "first EMG" response was the minimum stimulation amplitude at which EMG could be recorded from any muscle. In the legend of each panel, the mean and SD of each of the 3 parameters are given as calculated over the range of electrodes. Above each panel, the animal is named and indicated as being spinally intact (I) or chronically spinalized (S) and decerebrate (D). *A*: in chronically spinalized *cat R1,* sensory axons were always antidromically stimulated before MNs were activated. *B*: in chronically spinalized *cat R2,* sensory axons were always antidromically stimulated before MNs were activated, even with the deep electrodes in the ventral horn. *C*: in spinally intact *cat R3,* sensory axons were always antidromically stimulated before MNs were activated with the exception of the deepest electrode (E6) where the 1st EMG signal had a threshold of 31 μA and the 1st dorsal root ENG had a threshold of 36 μA. The thresholds for compound dorsal root action potentials and EMG were essentially the same for the 2nd deepest electrode (E5): 31 μA for the 1st ENG and 32.5 μA for the 1st EMG. *D*: in spinally intact *cat R4,* sensory axons were always antidromically stimulated before MNs were activated with the exception of the deepest electrode (E6).

to the ISMS array exhibited compound action potentials in response to stimulation through electrodes E2 and E5 at amplitudes from 50 to 100 μA, whereas the same rootlet only exhibited compound action potentials at stimulation amplitudes >200 μA with electrodes E1 and E6. Dorsal rootlets close to the site of ISMS exhibited compound action potentials within a much narrower range of stimulation amplitudes, presumably because of the higher density of collaterals in this region.

One obvious feature of Fig. 8*A* is the apparent asymmetry in the range and distribution of ISMS amplitudes which first elicited a dorsal root response. Dorsal rootlets rostral to the ISMS electrode maintained a relatively consistent distribution of thresholds beginning immediately rostral to the ISMS electrode. Caudal to the ISMS electrode, the dorsal rootlet thresholds were consistently low for *animals R2* and *R3*, but for *animals R1* and *R4* began to increase rapidly to over 200 μA beginning 7 mm caudal to the electrodes. This effect was primarily observed in *animal R4* where the examined rootlets were up to 17 mm caudal to the ISMS electrodes.

DISCUSSION

The main finding of this study was that sensory afferents were nearly always activated at lower ISMS thresholds than MNs (cell bodies or axons), whether the electrode tips were located in the dorsal horn, intermediate gray matter, or ventral horn. This is consistent with previous work showing that at low

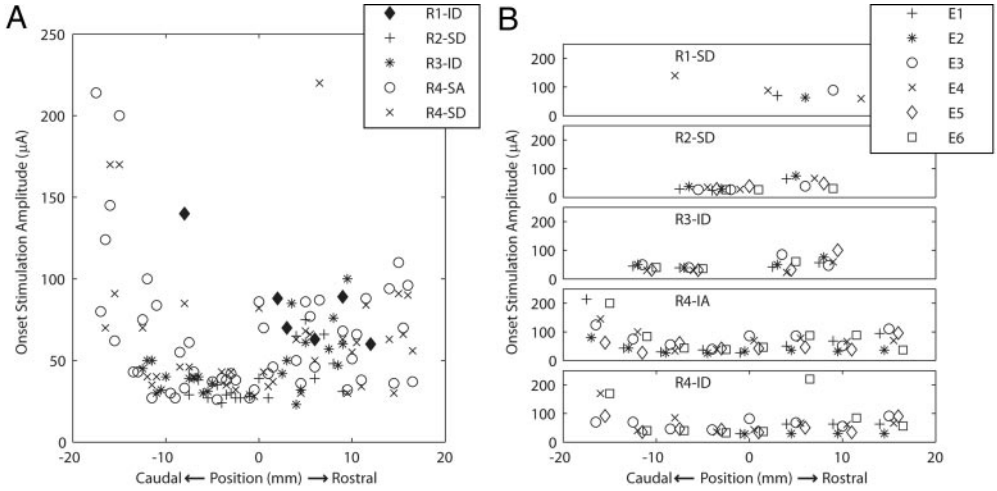

FIG. 8. Antidromic spread of activity through sensory axons in the spinal cord. The relationship between the minimum ISMS amplitude required to elicit a compound action potential in a specific dorsal root and the distance between the ISMS electrode and the dorsal root entry zone is shown. Compound dorsal root action potentials were recorded up to ±17 mm away from the stimulating electrode. Animals are listed (*R1–R4*) and indicated as being spinally intact (I) or chronically spinalized (S) and anesthetized (A) or decerebrate (D). *A*: pooled data from all 4 animals. All dorsal roots and electrodes are shown. *B*: same data as displayed in *A* but showing the rostrocaudal spread of activity from each stimulating electrode for each animal.

stimulation levels, ISMS activates MNs transsynaptically except when applied in close proximity to the initial segments of MN axons (Gustafsson and Jankowska 1976). What is new in this study is the demonstration of a very extensive spread of activity resulting from the antidromic activation of afferent axons with focal ISMS, especially with the ISMS electrodes in the ventral horn. Responses were detected in dorsal root filaments with entry zones 17 mm rostral and 17 mm caudal to a single microwire delivering ISMS pulses. This result suggests that when ISMS was applied at a given point within the gray matter of the spinal cord, antidromic action potentials were elicited in terminal branches of sensory afferents close to the electrode tip. These action potentials propagated back to their parent axons and via dorsal columns to dorsal root filaments, where our recording electrodes were located. In addition, the fact that many muscles showed responses at polysynaptic latencies, suggests that the action potentials also propagated rostrally and caudally along the dorsal columns and re-entered the gray matter at other collaterals of the afferents. Rootlets farther from the ISMS electrodes were not examined. This amount of stimulus spread is greater than the entire length of the lumbosacral enlargement (28.8 $\pm$ 2.4 mm) (Vanderhorst and Holstege 1997).

Horseradish peroxidase tracing studies by Brown (1981) have shown that sensory afferent collaterals can be found entering the spinal cord gray matter up to 10 mm rostrally and 5 mm caudally from their entry zones. The existence of afferent collaterals projecting from the L_{2-4} spinal segments to at least S_1 has also been demonstrated electrophysiologically (Wall and Werman 1976) and by axonal degeneration (Imai and Kusama 1969). Furthermore, branches of spindle afferents are known to synaptically excite most if not all homonymous MNs (Mendell and Henneman 1971). Also, dorsal horn interneurons respond to input from afferents with entry points up to three segments away (Mendell et al. 1978). These facts indicate that what is presumed to be focal stimulation of the spinal cord in fact probably excites both MNs and interneurons over large distances in all directions via antidromic activity in afferent fibers. In addition to the activation of sensory afferents, ISMS presumably recruits propriospinal axons in the vicinity of the electrode tips which may be important in contributing to the net motor output. Long-ranging propriospinal neurons with terminations in the lumbosacral enlargement are known to exist (Jankowska et al. 1974) but are unlikely to be the cause of the widespread activation of dorsal rootlets in this study.

These results were neither obvious to us in our own previous ISMS studies nor was the widespread activation of the spinal cord by ISMS recognized at the outset as a possible factor in the work that led to the hypothesis of movement primitives (Bizzi et al. 1991). Movement primitives have been observed after chronic deafferentation (Giszter et al. 1993; Tresch and Bizzi 1999), but the primitives themselves were somewhat changed from those observed with intact afferent input. ISMS, particularly in the dorsal horn and intermediate region, may also activate cutaneous nociceptive afferents that activate columnar somatotopically organized modules that coordinate the withdrawal reflex (Schouenborg 2003). The modules have been demonstrated in the rat (Schouenborg and Kalliomaki 1990; Schouenborg and Weng 1994; Schouenborg et al. 1992) and cat (Levinsson et al. 1999) and are present after spinalization, although the specificity of the receptive field mapping degrades over time (Schouenborg et al. 1992) The relationship between these reflex modules and the theory of movement primitives is unclear. These observations, in combination with our results of widespread activity caused by antidromically activated afferents suggests that the interpretation of the results of ISMS in the presence of intact afferent fibers is challenging. When afferent fibers are intact, the transsynaptic activation of MNs elicited by antidromic activation of sensory afferents in response to ISMS is bound to affect movements in a way that may not occur in the normally functioning nervous system. This could also partly explain the results of Mushahwar et al. (2004) in which ISMS in the intermediate gray matter elicited responses that were significantly modified by changes in descending input to the spinal cord caused by decerebration and acute spinalization.

The experimental demonstration that focal stimulation excites a whole population of axons at lower intensities than a co-localized population of neuronal cell bodies has broader implications. Currently, the mechanism by which deep brain stimulation operates is unknown (Dostrovsky and Lozano 2002). However, theoretical work (McIntyre and Grill 2000; McIntyre et al. 2004), experiments involving intracortical stimulation (Jankowska et al. 1975) and in vitro experimental data (Nowak and Bullier 1998) all suggest that electrical stimulation in the CNS, notably in the basal ganglia, excites axons at lower intensities than local neuronal cell bodies. To demonstrate this in vivo and to examine the relative recruitment of axons versus neuronal cell bodies, the neuroanatomy has to be such that there is separate electrophysiological access to the two populations. With current technology, this is probably only possible in the spinal cord, where the activity of afferent axons is selectively accessible in the dorsal roots, and the activity of MNs is selectively accessible either via their axons in the ventral roots or via the muscles to which they project. Our study strongly supports both the theoretical and experimental work suggesting that in the CNS, large populations of axons around a microelectrode are activated at lower thresholds than nearby cell bodies. Additionally, these results suggest that ISMS antidromically activates not only sensory axons but could also activate interneurons and en passant axons of other neurons that could in turn excite or inhibit neurons elsewhere in the network.

In addition to theoretical (McIntyre and Grill 2000) and experimental (Gustafsson and Jankowska 1976) evidence suggesting that axons are activated before cell bodies, one factor that might bias excitation toward the sensory axons in ISMS is the small number of MN cell bodies and axons close to a microwire tip compared with the number of afferents with branches in the same volume of gray matter. Given that a single MN receives synaptic input from many afferents, the density of terminal branches of afferent axons in any focal volume of ventral horn is sure to be much higher than the density of MNs. This might explain why MN cell bodies and their axons were usually excited at higher thresholds than sensory axons. It is also consistent with the observation that the difference between thresholds for dorsal root potentials and EMG was generally smaller when electrodes were positioned in the ventral horn. In two cases (see Fig. 7), the threshold for EMG detection was essentially equal to or even slightly below that for dorsal root potentials. At low stimulation amplitudes in the ventral horn, it is probable that MN axons rather than MN

cell bodies themselves were activated by electrical stimulation. In fact ISMS-elicited action potentials leading to short-latency EMG responses may have originated in the MN axons in all cases (Gustafsson and Jankowska 1976; McIntyre et al. 2004). Other factors that may bias excitation preferentially toward sensory axons rather than motor axons include the observed differences in the time constants of sensory and motor axons as well as primary afferent depolarization (PAD) caused by presynaptic inhibition. Erlanger and Blair (1938) first reported preferential activation of motor or sensory axons in the trunks of bullfrog spinal roots depending on the stimulation pulse width. At short pulse widths, motor axons were preferentially activated, whereas at longer pulse widths, sensory axons were preferentially activated. This phenomenon exists in human peripheral nerve as well, and Panizza et al. (1992) have demonstrated that the pulse widths at which the motor and sensory thresholds are equivalent in the ulnar and median nerves are 200 and 300 μs respectively. The reason for this difference has been postulated to be a higher percentage of persistent sodium channels at the nodes of Ranvier of sensory axons (Bostock and Rothwell 1997). Whether these effects are present in the spinal cord is unknown; however, the pulse width used in our experiments (200 μs) is in the range where differences between sensory and motor thresholds was minimal in peripheral nerves. PAD could also have an effect on the observed differences between sensory and motor activation thresholds (Rudomin and Schmidt 1999). PAD would bias activation thresholds toward lower sensory axon thresholds while also increasing the threshold for reflexly evoked motor activity.

In this study, single shocks were used, rather than trains of pulses as would typically be used in a neuroprosthesis application. Trains of pulses would have likely lowered the threshold for axonal activation (Gustafsson and Jankowska 1976) and would therefore have recruited both afferent axons, efferent axons and any transsynaptic efferent responses at lower stimulation amplitudes. Whether there might have been a differential effect on afferent or efferent axons with trains of pulses is unknown. However, because the microelectrode tips would most likely be near afferent or interneuronal axons rather than efferent cell bodies or axons, any effect of reduced thresholds would probably be most significant on afferent or interneuronal axons.

Given the increased afferent axon density in the dorsal horn and intermediate gray matter compared with the ventral horn (Brown 1981), one might predict that the threshold for detecting dorsal rootlet action potentials would be lower with stimulating electrodes located in these more dorsal regions. However, this was not observed. Differences in the dorsal rootlet ENG detection thresholds were observed with different electrodes but did not seem to correlate with electrode depth. Also, as mentioned previously, no relationship between the stimulating electrode depth and the dorsal rootlet ENG threshold at different rostrocaudal locations was found. This implies that electrodes in the dorsal horn and ventral horn are equally likely to elicit compound dorsal rootlet action potentials at various rostrocaudal locations. The fact that in some cases, larger stimulation amplitudes were required to elicit compound action potentials in dorsal rootlets farther from the site of ISMS suggests that the density of axon collaterals decreases (particularly in the rostral direction).

As the distance between the ISMS electrode and recording electrodes on a dorsal rootlets increased, a rostrocaudal asymmetry in the dorsal rootlet ENG threshold was observed. The reason for this asymmetry is unclear, although PAD mediated by centrally controlled presynaptic inhibition could conceivably cause these results. Lomeli et al. (1998) have demonstrated that lumbar segmental and ascending collaterals of the same primary afferent exhibit differing amounts of PAD as a result of centrally controlled presynaptic inhibition of the interneurons controlling PAD. Asymmetries between rostrally and caudally projecting collaterals have also been described in terms of conduction velocities (Wall 1994), but any relationship between this and the results observed in this study are unknown.

In addition to comparing dorsal root ENG and hindlimb muscle EMG onset latency differences, the progression of EMG onset latencies themselves provide insight into the recruitment of neurons with ISMS. At high stimulation amplitudes ($>$100 μA), the onset latency was generally on the order of 2–4 ms. However, at lower amplitudes, EMG onset latencies increased dramatically up to 14 ms. The maximum distance between intraspinal stimulating and EMG recording electrodes was on the order of 250 mm. Assuming the lowest reported cat MN conduction velocity of 60 mm/ms (Matthews 1972), a delay of 0.5 ms at the neuromuscular junction and a further delay of 0.5 ms for muscle fiber action potentials to be detected by EMG electrodes, only 5 ms are accounted for, providing an upper limit on what could be considered "direct" activation of MNs. Because EMG responses were frequently detected with onset latencies $>$5 ms, these responses must have been generated by the synaptic activation of MNs by afferent axons or axons of interneurons. This pattern of presumed synaptic activation of MNs occurred frequently when ISMS amplitudes were $<$100 μA. In cases where EMG onset latencies were very long (8–14 ms), polysynaptic transmission and possibly slowly conducting axons of afferents and interneurons are implicated. Because muscle fibers themselves conduct action potentials slowly ($\sim$4 mm/ms), a potential source of error in estimating latencies was the distance between the motor endplate zone and the nearest EMG electrode. However, the bipolar electrode configuration used is sensitive to potential changes occurring at a distance and given that EMG was reliably detected at minimal latencies of 2–4 ms in all recorded muscles at high stimulation amplitudes, the latency estimates were probably no more than 2 ms too large. These minima were assumed to represent direct motoneuronal activation.

One issue surrounding the use of ISMS for neuroprostheses is that of sensory perception. Activation of afferents and ascending tracts could potentially cause discomfort or pain. Although we did not examine what kinds of afferents were activated in our experiments, pain induced by ISMS was not observed in awake spinally intact cats with chronically implanted electrodes in the ventral horn (Mushahwar et al. 2000). The only human studies using ISMS, in which micturition was the desired outcome, excluded subjects with sensation below the level of spinal cord injury (Nashold et al. 1972, 1977). Given that the afferents activated by ISMS in intermediate and ventral gray matter are most likely large muscle afferents, the sensations evoked in incomplete spinal cord injury subjects would likely be similar to those evoked by peripheral nerve

neuroprostheses such as the BIONic WalkAid (Weber et al. 2005).

In previous ISMS studies with electrodes targeted to achieve functionally relevant hindlimb movements, stimulation amplitudes were generally in the range of 50–250 μA (Mushahwar et al. 2000). In our study, electrodes targeted the gray matter and were not positioned to elicit specific hindlimb movements, although the most ventral electrodes were near the regions of the spinal cord where such movements would be expected. Under these conditions and stimulation amplitudes in the range of 50–250 μA, most of the recorded muscles exhibited detectable activity. In *animal R3,* the three deepest electrodes coactivated the antagonistic pair LG and TA regardless of stimulation amplitude. In *animal R2,* at 100 μA, all of the ISMS electrodes caused contractions of LG, MG, SMa, BFp, and BFa: the entire set of recorded muscles. A similar pattern was observed in the other animals where recordable EMG activity was detected in nearly every muscle at stimulation amplitudes high enough to generate functional movement. Single-joint movements and multi-joint synergies (Mushahwar et al. 2000) as well as locomotor patterns (Guevremont et al. 2006) can be achieved with carefully positioned ISMS electrodes in the ventral horn. However, the present results suggest that stimulation at many locations in the gray matter produce widespread activation of many hindlimb muscles.

This experimental evidence has corroborated previous work, both experimental and theoretical, suggesting that within the CNS, axons are activated at lower thresholds than cell bodies. However, perhaps surprisingly, it was found that afferent axons were nearly always activated antidromically at lower thresholds than the large MN axons even when the stimulating electrodes were deep within the ventral horn. It was also demonstrated that the spread of activity within the spinal cord mediated by these afferent fibers can extend for at least 17 mm rostrally and caudally, covering the entire lumbosacral enlargement. This spread of activity activates large numbers of muscles and may explain some of the observations that led to the movement primitives hypothesis. Our results also help explain how ISMS activates large populations of neurons distributed over several spinal segments, and should be taken into account in the interpretation of results obtained with microstimulation within the CNS.

ACKNOWLEDGMENTS

The authors thank A. Denington for technical assistance.

GRANTS

This work was supported by the National Institute of Neurological Disorders and Stroke, Natural Sciences and Engineering Research Council of Canada and the Alberta Heritage Foundation for Medical Research.

REFERENCES

Barbeau H, McCrea DA, O'Donovan MJ, Rossignol S, Grill WM, and Lemay MA. Tapping into spinal circuits to restore motor function. *Brain Res Brain Res Rev* 30: 27–51, 1999.

Bizzi E, D'Avella A, Saltiel P, and Tresch M. Modular organization of spinal motor systems. *Neuroscientist* 8: 437–442, 2002.

Bizzi E, Giszter SF, Loeb E, Mussa-Ivaldi FA, and Saltiel P. Modular organization of motor behavior in the frog's spinal cord. *Trends Neurosci* 18: 442–446, 1995.

Bizzi E, Mussa-Ivaldi FA, and Giszter S. Computations underlying the execution of movement: a biological perspective. *Science* 253: 287–291, 1991.

Bostock H and Rothwell JC. Latent addition in motor and sensory fibres of human peripheral nerve. *J Physiol* 498: 277–294, 1997.

Brown AG. *Organization in the Spinal Cord: The Anatomy and Physiology of Identified Neurons.* Berlin: Springer, 1981.

Carter RR, McCreery DB, Woodford BJ, Bullara LA, and Agnew WF. Micturition control by microstimulation of the sacral spinal cord of the cat: acute studies. *IEEE Trans Rehabil Eng* 3: 206–214, 1995.

Dostrovsky JO and Lozano AM. Mechanisms of deep brain stimulation. *Mov Disord* 17, *Suppl* 3: S63–68, 2002.

Erlanger J and Blair EA. Comparitive observations on motor and sensory fibers with special reference to repetitiousness. *Am J Physiol* 121: 431–453, 1938.

Giszter SF, Mussa-Ivaldi FA, and Bizzi E. Convergent force fields organized in the frog's spinal cord. *J Neurosci* 13: 467–491, 1993.

Guevremont L, Renzi CG, Norton JA, Kowalczewski J, Saigal R, and Mushahwar VK. Locomotor-related networks in the lumbosacral enlargement of the adult spinal cat: activation through intraspinal microstimulation *IEEE Trans Neural Syst Rehab Eng*, 14: 266–272, 2006.

Gustafsson B and Jankowska E. Direct and indirect activation of nerve cells by electrical pulses applied extracellularly. *J Physiol* 258: 33–61, 1976.

Imai Y and Kusama T. Distribution of the dorsal root fibers in the cat. An experimental study with the Nauta method. *Brain Res* 13: 338–359, 1969.

Jankowska E, Lundberg A, Roberts WJ, and Stuart D. A long propriospinal system with direct effect on motoneurons and on interneurons in the cat lumbosacral cord. *Exp Brain Res* 21: 169–194, 1974.

Jankowska E, Padel Y, and Tanaka R. The mode of activation of pyramidal tract cells by intracortical stimuli. *J Physiol* 249: 617–636, 1975.

Jankowska E and Roberts WJ. An electrophysiological demonstration of the axonal projections of single spinal interneurons in the cat. *J Physiol* 222: 597–622, 1972.

Levinsson A, Garwicz M, and Schouenborg J. Sensorimotor transformation in cat nociceptive withdrawal reflex system. *Eur J Neurosci* 11: 4327–4332, 1999.

Loeb GE. Past the equilibrium point. *Behav Brain Sci* 15: 774–775, 1992.

Lomeli J, Quevedo J, Linares P, and Rudomin P. Local control of information flow in segmental and ascending collaterals of single afferents. *Nature* 395: 600–604, 1998.

Matthews PBC. *Mammalian Muscle Receptors and Their Central Actions.* London: Edward Arnold, 1972.

McCreery D, Pikov V, Lossinsky A, Bullara L, and Agnew W. Arrays for chronic functional microstimulation of the lumbosacral spinal cord. *IEEE Trans Neural Syst Rehabil Eng* 12: 195–207, 2004.

McIntyre CC and Grill WM. Selective microstimulation of central nervous system neurons. *Ann Biomed Eng* 28: 219–233, 2000.

McIntyre CC, Grill WM, Sherman DL, and Thakor NV. Cellular effects of deep brain stimulation: model-based analysis of activation and inhibition. *J Neurophysiol* 91: 1457–1469, 2004.

Mendell LM and Henneman E. Terminals of single Ia fibers: location, density, and distribution within a pool of 300 homonymous motoneurons. *J Neurophysiol* 34: 171–187, 1971.

Mendell LM, Sassoon EM, and Wall PD. Properties of synaptic linkage from long ranging afferents onto dorsal horn neurones in normal and deafferented cats. *J Physiol* 285: 299–310, 1978.

Mushahwar V, Prochazka A, Ellaway PH, Guevremont L, and Gaunt RA. Microstimulation in CNS excites axons before neuronal cell bodies. *Soc Neurosci Abstr* 2003.

Mushahwar VK, Aoyagi Y, Stein RB, and Prochazka A. Movements generated by intraspinal microstimulation in the intermediate gray matter of the anesthetized, decerebrate, and spinal cat. *Can J Physiol Pharmacol* 82: 702–714, 2004.

Mushahwar VK, Collins DF, and Prochazka A. Spinal cord microstimulation generates functional limb movements in chronically implanted cats. *Exp Neurol* 163: 422–429, 2000.

Mushahwar VK and Horch KW. Proposed specifications for a lumbar spinal cord electrode array for control of lower extremities in paraplegia. *IEEE Trans Rehabil Eng* 5: 237–243, 1997.

Mushahwar VK and Horch KW. Selective activation and graded recruitment of functional muscle groups through spinal cord stimulation. *Ann N Y Acad Sci* 860: 531–535, 1998.

Nashold BS Jr, Friedman H, Glenn JF, Grimes JH, Barry WF, and Avery R. Electromicturition in paraplegia. Implantation of a spinal neuroprosthesis. *Arch Surg* 104: 195–202, 1972.

Nashold BS Jr, Grimes J, Friedman H, Semans J, and Avery R. Electrical stimulation of the conus medullaris in the paraplegic. A 5-year review. *Appl Neurophysiol* 40: 192–207, 1977.

Nowak LG and Bullier J. Axons, but not cell bodies, are activated by electrical stimulation in cortical gray matter. I. Evidence from chronaxie measurements. *Exp Brain Res* 118: 477–488, 1998.

Panizza M, Nilsson J, Roth BJ, Basser PJ, and Hallett M. Relevance of stimulus duration for activation of motor and sensory fibers: implications for the study of H-reflexes and magnetic stimulation. *Electroencephalogr Clin Neurophysiol* 85: 22–29, 1992.

Ranck JB Jr. Which elements are excited in electrical stimulation of mammalian central nervous system: a review. *Brain Res* 98: 417–440, 1975.

Renshaw B. Activity in the simplest spinal reflex pathways. *J Neurophysiol* 3: 373–387, 1940.

Roberts WJ and Smith DO. Analysis of threshold currents during microstimulation of fibres in the spinal cord. *Acta Physiol Scand* 89: 384–394, 1973.

Rudomin P and Schmidt RF. Presynaptic inhibition in the vertebrate spinal cord revisited. *Exp Brain Res* 129: 1–37, 1999.

Saltiel P, Wyler-Duda K, D'Avella A, Tresch MC, and Bizzi E. Muscle synergies encoded within the spinal cord: evidence from focal intraspinal NMDA iontophoresis in the frog. *J Neurophysiol* 85: 605–619, 2001.

Schouenborg J. Somatosensory imprinting in spinal reflex modules. *J Rehabil Med*: 73–80, 2003.

Schouenborg J, Holmberg H, and Weng HR. Functional organization of the nociceptive withdrawal reflexes. II. Changes of excitability and receptive fields after spinalization in the rat. *Exp Brain Res* 90: 469–478, 1992.

Schouenborg J and Kalliomaki J. Functional organization of the nociceptive withdrawal reflexes. I. Activation of hindlimb muscles in the rat. *Exp Brain Res* 83: 67–78, 1990.

Schouenborg J and Weng HR. Sensorimotor transformation in a spinal motor system. *Exp Brain Res* 100: 170–174, 1994.

Snow S, Horch KW, and Mushahwar VK. Intraspinal microstimulation using cylindrical multielectrodes. *IEEE Trans Biomed Eng* 53: 311–319, 2006.

Tresch MC and Bizzi E. Responses to spinal microstimulation in the chronically spinalized rat and their relationship to spinal systems activated by low threshold cutaneous stimulation. *Exp Brain Res* 129: 401–416, 1999.

Vanderhorst VG and Holstege G. Organization of lumbosacral motoneuronal cell groups innervating hindlimb, pelvic floor, and axial muscles in the cat. *J Comp Neurol* 382: 46–76, 1997.

Wall PD. Impulses in the rostral branch of primary afferents in rat dorsal columns travel faster than those in the caudal branch. *Neurosci Lett* 165: 75–78, 1994.

Wall PD and Werman R. The physiology and anatomy of long ranging afferent fibres within the spinal cord. *J Physiol* 255: 321–334, 1976.

Weber DJ, Stein RB, Chan KM, Loeb G, Richmond F, Rolf R, James K, and Chong SL. BIONic WalkAide for correcting foot drop. *IEEE Trans Neural Syst Rehabil Eng* 13: 242–246, 2005.